OPERATION and PROPOSALS

1. Outline of the Accelerators

Two electron storage rings, the PF ring and PF-AR, have been operated as dedicated light sources at Photon Factory. Simultaneous and continuous injections to the four different rings (the PF ring, PF-AR, SuperKEKB HER, and LER) from the KEK linear accelerator (LINAC) were completed in the second half of FY2018. The user operation of both light sources is performed with full top-up injection. For PF-AR, a new operation mode of 5 GeV was introduced from the beginning of FY2019. The low-energy operation is planned to save electricity costs and to maximize the operation time on a tight budget. It was confirmed that the electricity cost could be reduced by 40% by lowering the stored energy to 5 GeV from 6.5 GeV. By operating half of the total time at 5 GeV in FY2019, the operation time of PF-AR was successfully increased by about 25% compared to the previous year.

The machine parameters of the rings and the calculated spectral performances are listed in **Tables 1** and **2**. The spectral distributions of synchrotron radiation (SR) from the bending magnets and the insertion devices are shown in **Fig. 1**.

Table 1: Principal beam parameters of the PF ring and PF-AR.

	PF ring	PF-AR	
Energy	2.5 GeV	6.5 GeV	5 GeV
Natural emittance	34.6 nm rad	290 nm rad	170 nm rad
Circumference	187 m	377 m	←
RF frequency	500.1 MHz	508.6 MHz	←
Bending radius	8.66 m	23.7 m	←
Energy loss per turn	0.4 MeV	6.66 MeV	2.33MeV
Damping time			
Vertical	7.8 ms	2.5 ms	5.4 ms
Longitudinal	3.9 ms	1.2 ms	2.7 ms
Natural bunch length	10 mm	16 mm	15mm
Momentum compaction factor	0.00644	0.0126	←
Natural chromaticity			
Horizontal	–12.9	–13.6	←
Vertical	–17.3	–13.3	←
Stored current	450 mA	60 mA	←
Normal filling	250 bunches	Single	←
Beam lifetime	20 h (at 450 mA)	14 h (at 50 mA)	7 h (at 50 mA)
Hybrid filling	Single (50 mA) + 131 bunches (400 mA)		
Beam lifetime	8 h (450 mA)		

Table 2: Calculated spectral performances of the bending source and all the insertion devices at the PF ring (2.5 GeV, 450 mA) and PF-AR (6.5 GeV, 60 mA).

Name	*E/I* GeV/mA	λ_u cm	*N*	*L* m	$G_y(G_x)$ cm	$B_y(B_x)$ T	Type of magnet	σ_x mm	σ_y mm	$\sigma_{x'}$ mrad	$\sigma_{y'}$ mrad	$K_y(K_x)$	$\varepsilon_1/\varepsilon_c$ keV	*D*	*B*	P_T kW
PF	**2.5/450**															
Bend								0.41	0.059	0.178	0.012		4	5.38E+13	3.48E+14	
SGU#01		1.2	39	0.5	0.4	0.7	P(NdFeB)	0.6	0.012	0.088	0.029	0.78		4.56E+16	9.90E+17	0.4
U#02-1		6	60	3.6	2.8	0.4	H(NdFeB)	0.65	0.042	0.054	0.008	2.3		2.73E+17	1.55E+18	1.07
U#02-2		16	17	2.72	2.6	0.33(0.33)	P(NdFeB)	0.65	0.042	0.054	0.008	4.93(4.93)		9.53E+15	4.58E+16	0.53
SGU#03		1.8	26	0.5	0.4	1	P(NdFeB)	0.6	0.012	0.088	0.029	1.68		2.50E+16	5.44E+17	0.82
MPW#05-W		12	21	2.5	2.64	1.4	H(NdFeB)	0.71	0.045	0.078	0.009	16	5.9	2.22E+15	1.10E+16	8.83
U#13		7.6	47	3.6	2.3	0.68(0.34)	P(NdFeB)	0.74	0.02	0.094	0.019	4.84(2.42)		6.85E+16	4.70E+17	3.7
VW#14					5	5	S.C.	0.53	0.045	0.128	0.008		20.8	5.42E+13	3.59E+14	
SGU#15		1.76	27	0.5	0.4	0.97	P(NdFeB)	0.6	0.012	0.088	0.029	1.37		4.38E+15	9.44E+16	0.75
U#16-1 & 16-2		5.6	44	2.5	2.1	0.6(0.38)	P(NdFeB)	0.654	0.042	0.055	0.008	3(2)		1.42E+17	7.87E+17	2.2
SGU#17		1.6	29	0.5	0.4	0.92	P(NdFeB)	0.6	0.012	0.088	0.029	1.37		7.88E+15	1.71E+17	0.69
U#19		6.8	55	3.74	2.4	0.71(0.46)	P(NdFeB)	0.71	0.045	0.078	0.009	4.5(2.92)		1.14E+17	5.08E+17	4.76
U#28		16	22	3.52	2.7	0.33(0.33)	P(NdFeB)	0.53	0.045	0.127	0.008	4.93(4.93)		1.39E+16	6.59E+16	1.36
PF-AR	**6.5/60**															
Bend								1	0.2	0.593	0.036		26	3.90E+13	3.11E+13	
EMPW#NE01-W		16	21	3.36	3(11)	1(0.2)	P(NdFeB)	1.07	1.07	0.268	0.032	15(3)	28(90%)	1.84E+15	2.54E+15	5.52
U#NE03		4	90	3.6	1	0.8	P(NdFeB)	1.57	0.17	0.312	0.029	3		1.29E+16	7.66E+15	3.708
U#NW02		4	90	3.6	1	0.8	P(NdFeB)	1.57	0.17	0.312	0.029	3		1.29E+16	7.66E+15	3.708
U#NW12		4	95	3.8	1	0.8	P(NdFeB)	1.57	0.17	0.312	0.029	3		1.29E+16	7.66E+15	3.912
U#NW14-36		3.6	79	2.8	1	0.8	P(NdFeB)	1.35	0.14	0.338	0.036	2.8		7.69E+15	6.49E+15	3.12
U#NW14-20		2	75	1.5	0.8	0.63	P(NdFeB)	0.75	0.07	0.383	0.038	1.17		7.69E+15	6.49E+15	0.936

λ_u: period length, *N*: number of periods, *L*: length of undulator or wiggler, $G_y(G_x)$: minimum vertical (horizontal) gap height, $B_y(B_x)$: maximum vertical (horizontal) magnetic field, H: hybrid configuration, S.C.: superconducting magnet, σ_x, σ_y: horizontal or vertical beam size, $\sigma_{x'}$, $\sigma_{y'}$: horizontal or vertical beam divergence, $K_y(K_x)$: vertical (horizontal) deflection parameter, *D*: photon flux density (photons/sec/mrad^2/0.1%b.w.), *B*: brilliance (photons/sec/mm^2/mrad^2/0.1%b.w.), P_T:total radiated power. MPW#05 and EMPW#NE01 are operated in wiggler mode denoted by -W.

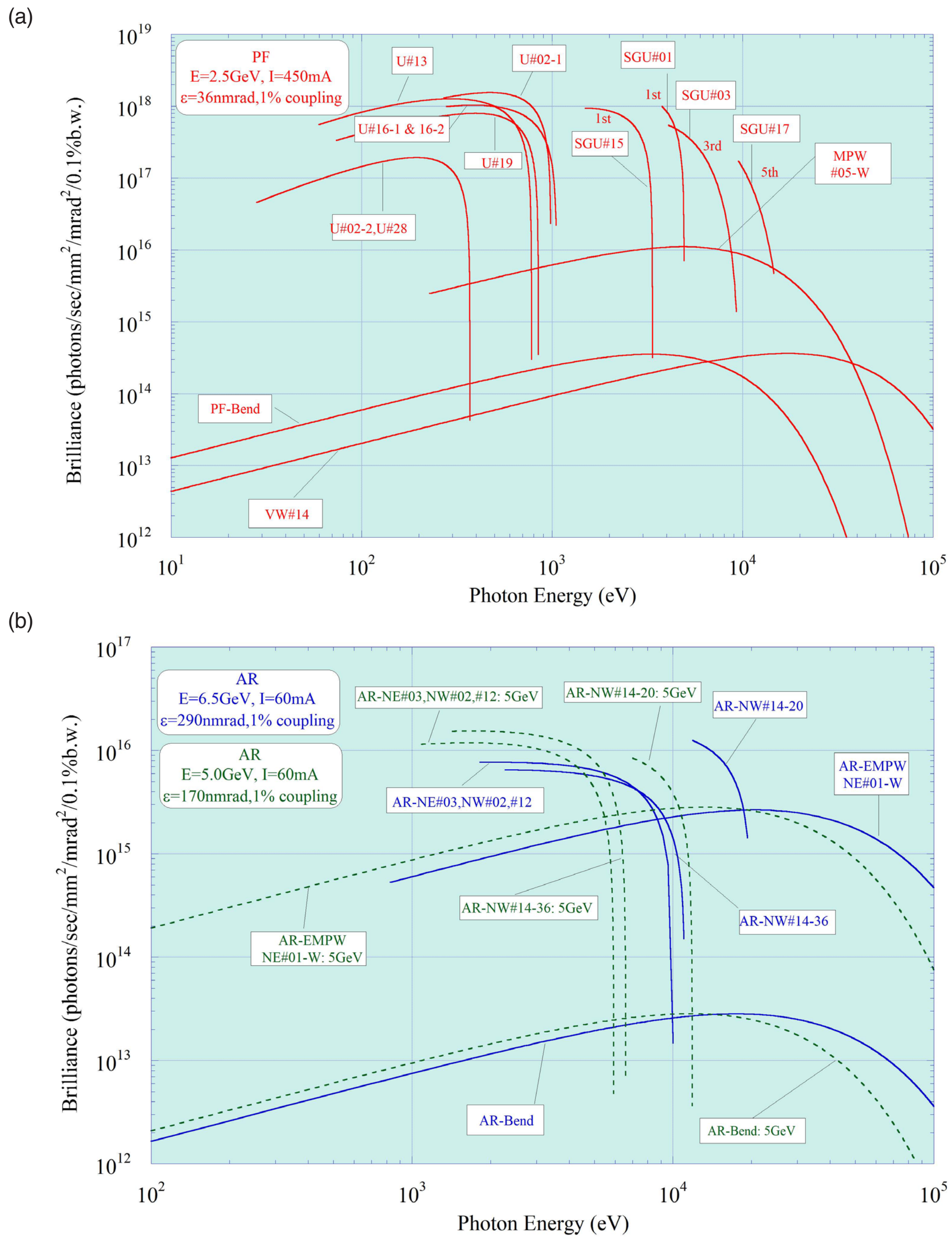

Figure 1: Synchrotron radiation spectra available at the Photon Factory. (a) PF ring, and (b) PF-AR, blue curves for 6.5 GeV and green dashed curves for 5 GeV. The name of each source is listed in **Table 2**. The spectral curve of each undulator is the locus of the peak of the first harmonic within the allowance range of K parameter. For SGU#01 and SGU#15, the first harmonic regions are shown. For SGU#03, the third harmonic region is shown. For SGU#17, the fifth harmonic region is shown.

2. Operation Summary

The operation schedule of the PF ring and PF-AR in FY2019 is shown in **Fig. 2**. The statistics of the accelerator's operation for the past decade are shown in **Fig. 3**. For the PF ring, to secure 3,000 hours of user operation time, the total operation time of about 3,500 hours has been maintained for the past few years. The operation time of PF-AR in FY2019 was about 25% higher than in the previous year due to the introduction of 5 GeV operation described above.

Detailed operation statistics and the number of failures from FY2010 to FY2019 are listed in **Table 3** for the PF ring. A breakdown of the total downtime in FY2019 is shown in **Fig. 4**. We apologize that there was a totalization error in the operation time in the PF Highlights last year; we have corrected the total operation time for FY2018 from 3,696 hours to 3,408 hours, and the scheduled use time from 3,120 hours to 2,832 hours as shown in **Table 3**.

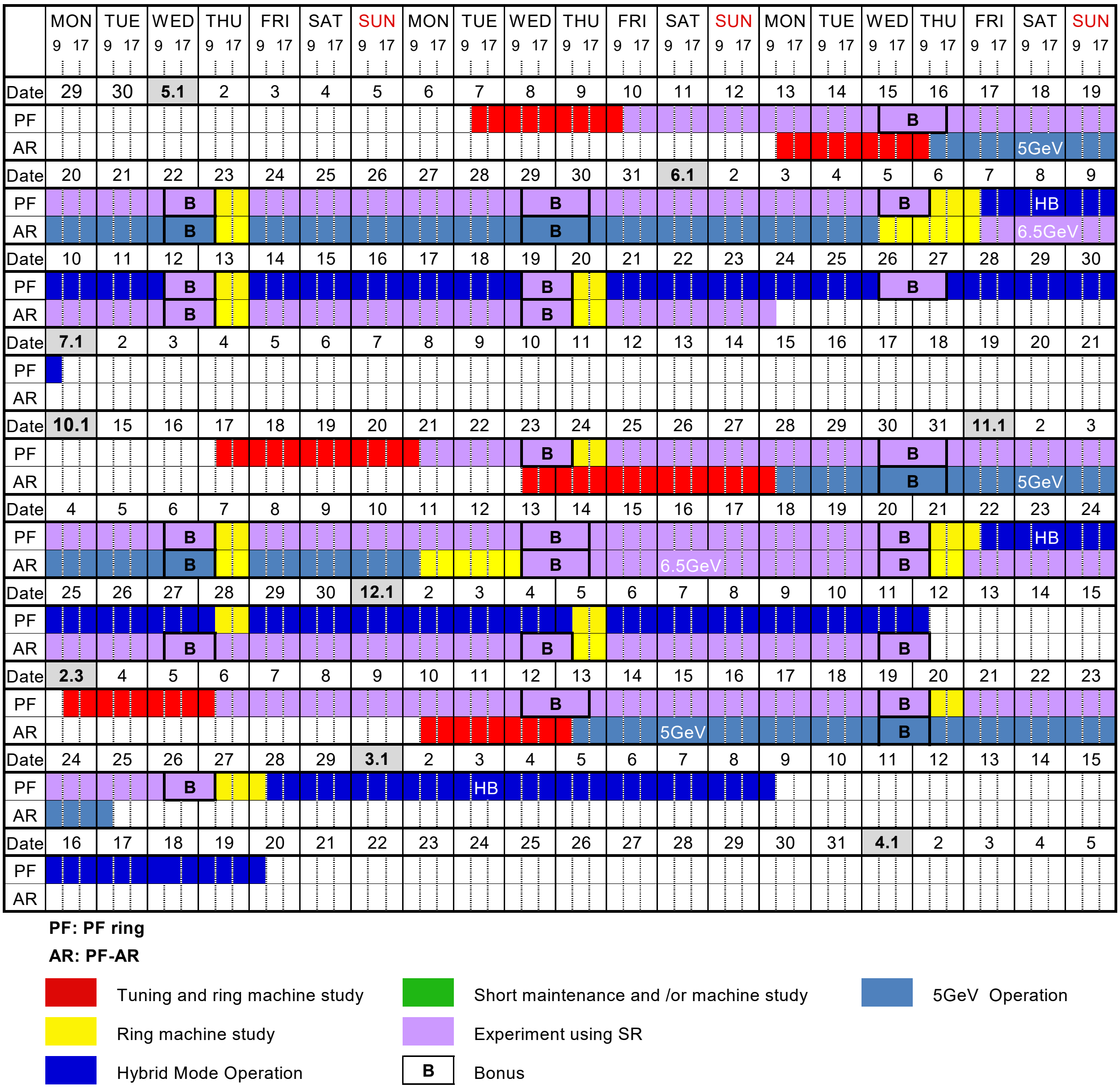

Figure 2: Operation schedule of PF ring and PF-AR in FY2019.

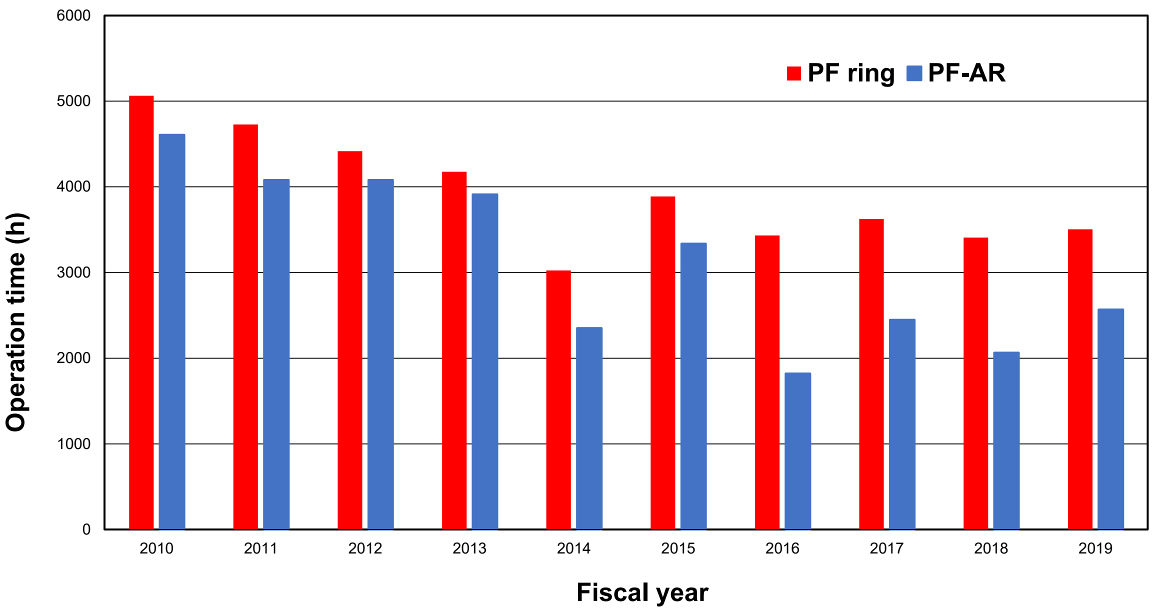

Figure 3: Total operation time for PF ring and PF-AR.

The total downtime was about twice that in previous years. This was due to frequent failures of the quadrupole magnet power supplies, which took a long time to recover. The downtime assigned to the magnet in **Fig. 4** accounts for about 70%. There used to be ten power supplies that had been manufactured in the 1990s, about 30 years ago. Two of them were updated in FY2019, but the other eight continue to be used. Because the manufacturers can no longer supply spare parts, it is essential to update these power supplies for stable operation of the PF ring.

We are developing a novel injection scheme using a multi-pole magnet instead of a set of conventional bump kicker magnets. The sextupole magnet shown on the right side of **Fig. 5** is currently installed in the PF ring. It is an improved version of the first model with a circular opening shown in the left of the figure. A large field gradient can be generated by narrowing the vertical aperture. However, contrary to our expectations, we could not obtain satisfactory injection efficiency using the improved model. It was speculated that the cause was eddy currents generated in the thin metal film coated inside the ceramic duct. In order to solve this problem, we have devised an inner surface coating to suppress the generation of eddy currents. The new ceramic duct was manufactured in FY2019, and we are going to install it at the beginning of FY2020.

The renewal of an aged septum magnet of the in-vacuum type, which has had a fatal water leak since FY2015, is also in progress. The new septum chamber will be installed in the injection section with a new septum magnet of the out-vacuum type during the 2020 summer shutdown. We expect to improve the injection efficiency and stability by optimizing the injection scheme associated with the reconstruction.

For PF-AR, detailed operation statistics and the number of failures from FY2010 to FY2019 are listed in **Table 4**. A breakdown of the total downtime in FY2019 is shown in **Fig. 6**.

The number of failures was less than half that in the previous year. The total downtime also fell to about half. The mean time between failures (MTBF) was the longest ever. These good results are considered to be due to stabilizing the stored current by the full-time top-up injection, and to maintaining the DC magnet power source in good condition. A further reason is the considerable decrease in the number of beam dumps attributed to dust tapping.

Table 3: Operation statistics for the PF ring from FY2010 to FY2019.

Fiscal Year	2010	2011	2012	2013	2014	2015	2016	2017	2018	2019
Total operation time (h)	5064	4728	4416	4176	3024	3888	3432	3624	3408	3504
Scheduled user time (h)	4080	2832	3792	3504	2328	3048	2928	3000	2832	3064
Ratio of user time (%)	80.6	59.9	85.9	83.9	77.0	78.4	85.3	82.8	83.1	87.4
No. of failures	18	18	23	22	15	23	18	14	17	20
Total down time (h)	29.2	14.9	37.6	52.1	11.4	14.4	17.3	16.6	28.4	59.9
Failure rate (%)	0.7	0.5	1.0	1.5	0.5	0.5	0.6	0.6	0.9	2.0
MTBF (h)	226.7	157.3	164.9	159.3	155.2	132.5	162.7	214.3	183.5	153.2
Mean down time (h)	1.6	0.8	1.6	2.4	0.8	0.6	1.0	1.2	1.7	3.0

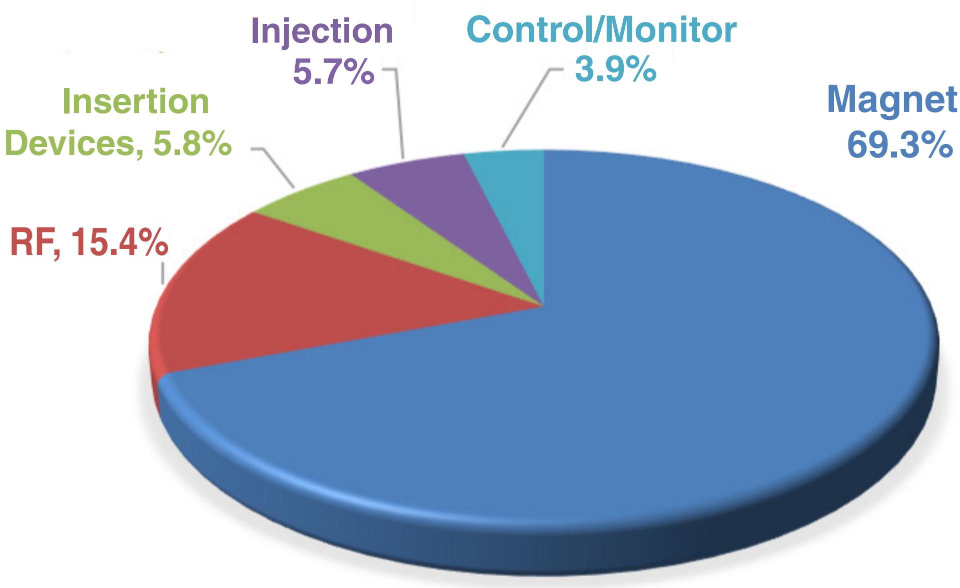

Figure 4: Breakdown of the total down time, 59.9 hours, for the PF ring in FY2019.

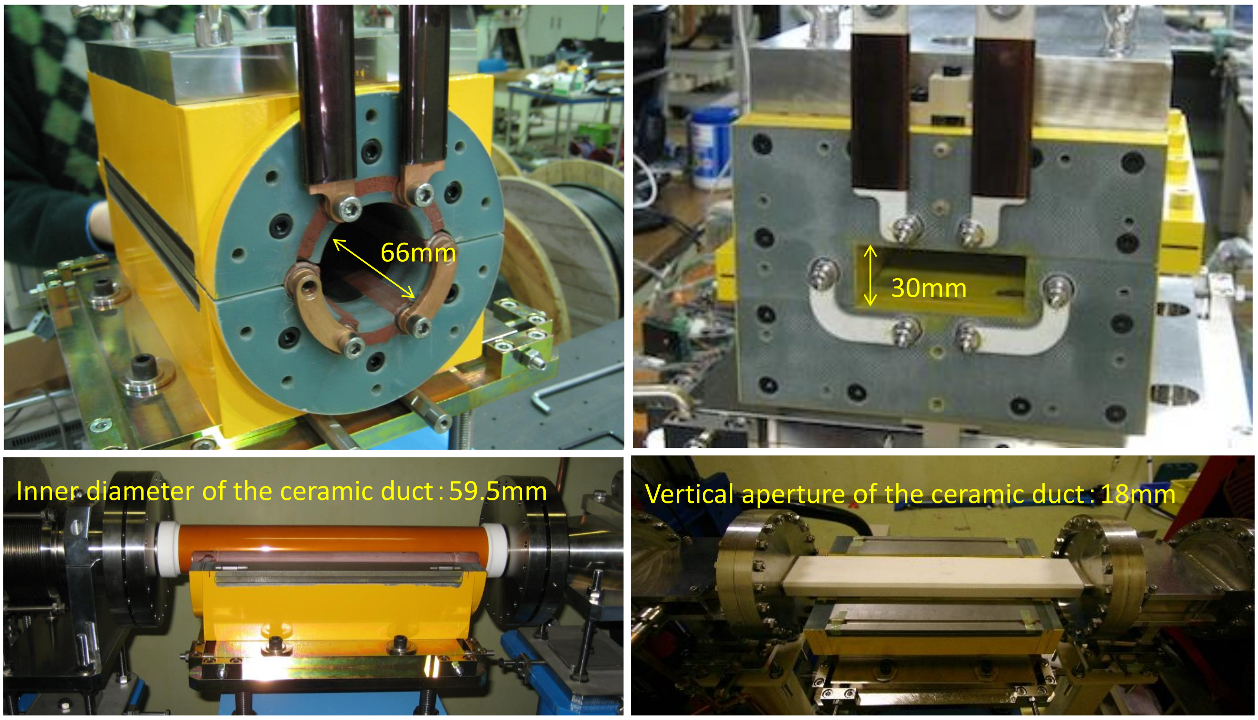

Figure 5: Original (left) and the updated (right) models of the pulsed sextupole magnets installed in the PF ring.

Table 4: Operation statistics for PF-AR from FY2010 to FY2019.

Fiscal Year	2010	2011	2012	2013	2014	2015	2016	2017	2018	2019
Total operation time (h)	4608	4080	4080	3912	2352	3336	1821	2448	2064	2568
Scheduled user time (h)	4032	2904	3672	3478	1992	2784	1104	2136	1608	2112
Ratio of user time (%)	87.5	71.2	90	88.9	84.7	83.5	60.6	87.3	77.9	82.2
No. of failures	74	49	33	47	22	18	13	55	25	8
Total down time (h)	73.7	38.7	29.7	99.6	37	31	18.3	24.7	26.4	12.3
Failure rate (%)	1.8	1.3	0.8	2.9	1.9	1.1	1.7	1.2	1.6	0.6
MTBF (h)	54.5	59.3	111.3	74	90.5	154.7	84.9	38.8	64.3	264.0
Mean down time (h)	1	0.8	0.9	2.1	1.7	1.7	1.4	0.4	1.1	1.5

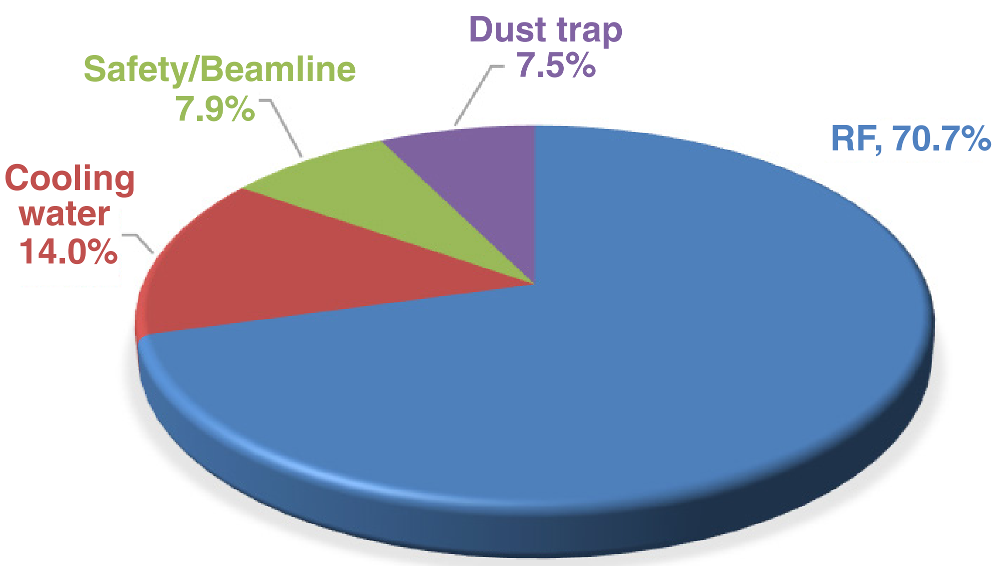

Figure 6: Breakdown of the total down time, 12.3 hours, for PF-AR in FY2019.

As in the previous year, beam dumps occurred several times caused by the temperature interlock of cables for extracting and damping the higher-order modes (HOMs) of acceleration cavities. The heating was considered to be due to aging and deterioration by radiation. Failures had been gradually increasing as the average stored current increased by the full-time top-up injection. As shown in **Fig. 7**, a multi-cell cavity called "APS cavity" is used for RF acceleration. Each APS cavity consists of 11 cavities. A set of HOM coupler, corrugated coaxial cable, and 3-kW dummy load is connected to each acceleration cavity. PF-AR has six units of APS cavities in total, so the total number of HOM couplers, cables, and dummy loads amounts to about 70 sets. During the 2019 summer shutdown, all of the HOM cables were replaced with new ones. Deteriorated polyethylene insulators inside the HOM couplers and the dummy loads were all replaced.

In recent years, the PF-AR operation time has been much less than the target of 3,000 hours. As its operating cost, mainly for electricity, is twice that of the PF ring, the budget shortage severely affected PF-AR. In FY2019, PF-AR was operated at a reduced energy of 5 GeV for about half of the total operation time. The electric power consumption at 5 GeV has been confirmed to be around 60% of that at 6.5 GeV. The operation time was thus extended by 25% compared to the previous year without increasing the operating cost. The 5-GeV operation will continue as an effective measure to extend the operation time. For 5 GeV injection, it is necessary to change the current of a DC bending magnet in the beam transport (BT) line to switch the 2.5-GeV beam of the PF ring and 5-GeV beam of PF-AR, so the top-up injection to the two rings is performed by time-sharing. It is a challenge to realize complete simultaneous injection by introducing a pulse magnet in the BT line or by taking other measures.

Figure 7: HOM couplers, HOM cables and dummy loads connected to the APS cavity of PF-AR.

3. Experimental Stations

Fifty-three experimental stations are in operation at the PF ring, PF-AR and slow positron facility (SPF), as shown in **Figs. 8**, **9** and **10**. Thirty-five stations are dedicated to research using hard X-rays, 14 stations for studies in the VUV and soft X-ray energy regions, and 4 stations for studies using slow positrons. **Tables 7**, **8** and **9** summarize the areas of research being carried out at the experimental stations at the PF ring, PF-AR and SPF.

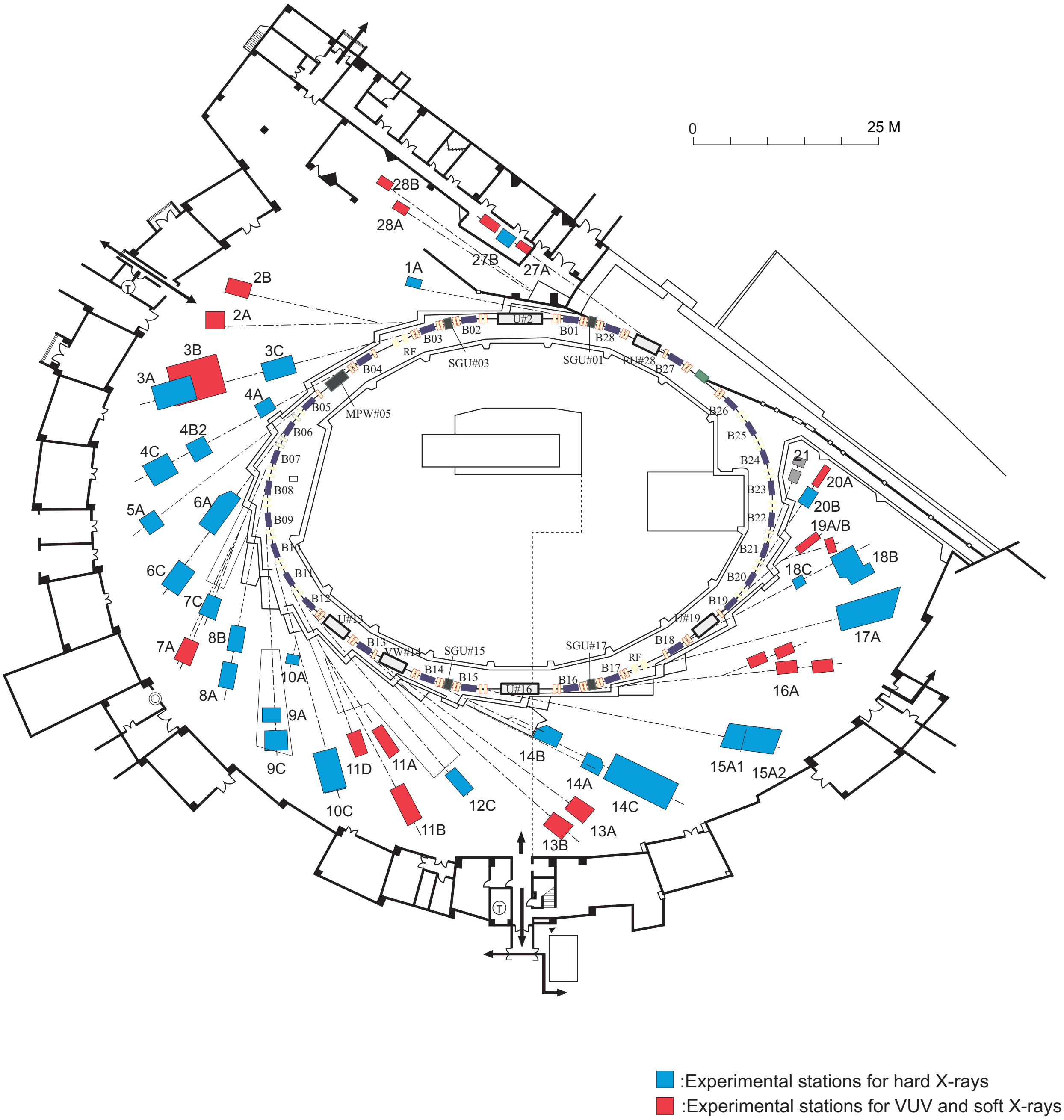

Figure 8: Plan view of the PF experimental hall, showing hard X-ray experimental stations (blue), and VUV and soft X-ray experimental stations (red).

Table 7: List of the experimental stations available for users at the PF ring.

Experimental Station		Person in Charge
BL-1	(Short Gap Undulator)	
A	Macromolecular crystallography	N. Matsugaki
BL-2	(Variable Polarization Undulator for VUV and planer undulator for SX)	
A	High-resolution VUV-SX beamline for angle-resolved photoemission spectroscopy	K. Horiba
B	High-resolution VUV-SX spectroscopies	K. Horiba
BL-3	(A: Short Gap Undulator)	
A	X-ray diffraction for material structural science	H. Nakao
B	VUV and soft X-ray spectroscopy (♠)	K. Edamoto [Rikkyo Univ.], J. Yoshinobu [The Univ. of Tokyo], K. Mase
C	Characterization of X-ray optical elements/White X-ray magnetic diffraction	K. Hirano
BL-4		
A	Trace element analysis, X-ray microprobe (♠)	Y. Takahashi [The Univ. of Tokyo], M. Kimura, Y. Niwa
B2	High resolution powder diffraction (♠)	H. Uekusa [Tokyo Tech.], H. Nakao
C	X-ray diffraction for material structural science	H. Nakao
BL-5	(Multipole Wiggler)	
A	Macromolecular crystallography	N. Matsugaki
BL-6		
A	Small-angle X-ray scattering	N. Igarashi
C	X-ray diffraction and spectroscopy (♠)	N. Happo [Hiroshima City Univ.], H. Nakao
BL-7		
A	Soft X-ray spectroscopy (♦)	J. Okabayashi [RCS, The Univ. of Tokyo], K. Amemiya
C	X-ray spectroscopy and diffraction	H. Sugiyama
BL-8		
A	Weissenberg camera for powder/Single-crystal measurements under extreme conditions	H. Sagayama
B	Weissenberg camera for powder/Single-crystal measurements under extreme conditions	H. Sagayama
BL-9		
A	XAFS	H. Abe
C	XAFS	H. Abe
BL-10		
A	X-ray diffraction and scattering (♠)	A. Yoshiasa [Kumamoto Univ.], R. Kumai
C	Small-angle X-ray Scattering	N. Shimizu
BL-11		
A	Soft X-ray spectroscopy	Y. Kitajima
B	Soft X-ray spectroscopy	Y. Kitajima
D	Characterization of optical elements used in the VSX region	K. Mase
BL-12		
C	XAFS	H. Nitani

Experimental Station		Person in Charge
BL-13	(Variable Polarization Undulator)	
A/B	VUV and soft X-ray spectroscopies with circular and linear polarization	K. Mase
BL-14	(Vertical Wiggler)	
A	Crystal structure analysis and detector development	S. Kishimoto
B	High-precision X-ray optics	K. Hirano
C	Medical applications and general purpose (X-ray)	K. Hyodo
BL-15	(Short Gap Undulator)	
A1	Semi-microbeam XAFS	Y. Takeichi
A2	High brilliance small-angle X-ray scattering	N. Shimizu
BL-16	(Variable Polarization Undulator)	
A	Soft X-ray spectroscopies with circular and linear polarization	K. Amemiya
BL-17	(Short Gap Undulator)	
A	Macromolecular crystallography	Y. Yamada
BL-18		
B	Multipurpose monochromatic hard X-ray station (♦)	G. Manna [SINP], R. Kumai
C	High pressure X-ray powder diffraction (DAC) (♠)	H. Kagi [The Univ. of Tokyo], N. Funamori
BL-19	(Variable Polarization Undulator)	
A/B	Soft X-ray microscopy and spectroscopy	K. Ono
BL-20		
A	VUV spectroscopy (◊)	M. Kitajima [Tokyo Tech], J. Adachi
B	White & monochromatic X-ray topography and X-ray diffraction experiment	H. Sugiyama
BL-27	(Beamline for radioactive samples)	
A	Radiation biology, soft X-ray photoelectron spectroscopy	A. Yokoya [QST], Y. Okamoto [JAEA], N. Usami
B	Radiation biology, XAFS	A. Yokoya [QST], Y. Okamoto [JAEA], N. Usami
BL-28	(Variable Polarization Undulator)	
A	High-resolution angle-resolved photoemission spectroscopy with circular and linear polarization	K. Horiba
B	High-resolution VUV spectroscopies with circular and linear polarization	K. Horiba

♠ User group operated beamline
♦ External beamline
◊ Operated by University

RCS: Research Center for Spectrochemistry, the University of Tokyo
JNCASR: Jawaharlal Nehru Centre for Advanced Scientific Research

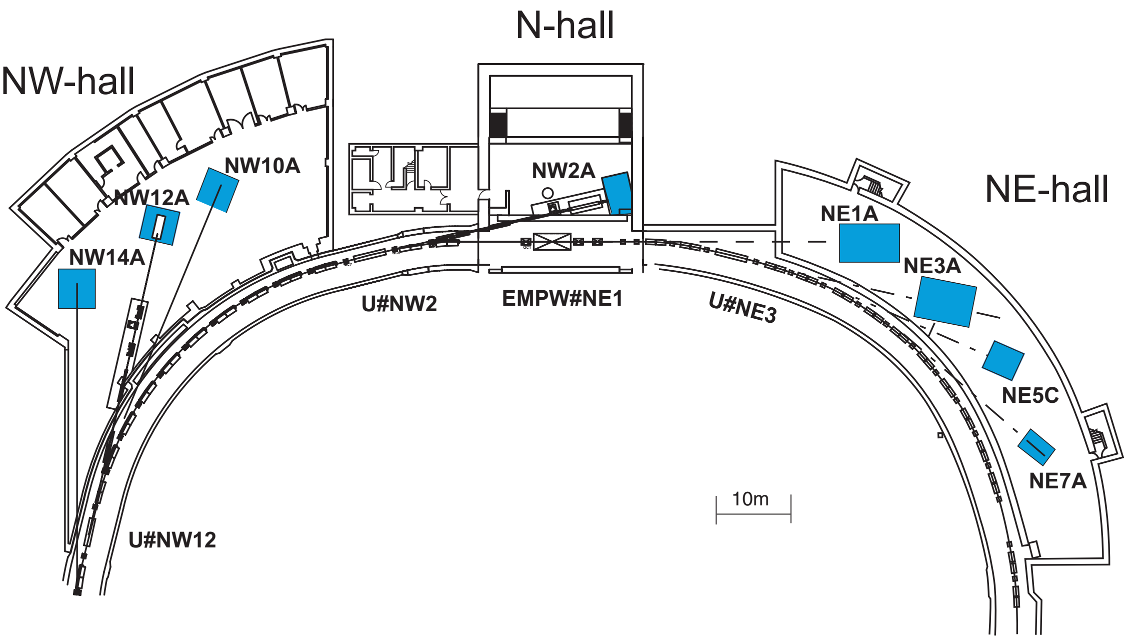

Figure 9: Plan view of the beamlines in the PF-AR north-east, north, and north-west experimental halls.

Table 8: List of the experimental stations at PF-AR.

Experimental Station		Person in Charge
AR-NE1	(Multipole Wiggler)	
A	Laser-heating high pressure X-ray diffraction and nuclear resonant scattering (DAC)	N. Funamori
AR-NE3	(In-vacuum Undulator)	
A	Macromolecular crystallography	Y. Yamada
AR-NE5		
C	High pressure and high temperature X-ray diffraction (MAX-80)	N. Funamori
AR-NE7		
A	High pressure and high temperature X-ray diffraction (MAX-III) (♥), X-ray imaging	K. Hyodo, T. Kubo [Kyusyu Univ.]
AR-NW2	(In-vacuum Type Tapered Undulator)	
A	Time-resolved Dispersive XAFS/XAFS/X-ray Diffraction	Y. Niwa
AR-NW10		
A	XAFS	H. Nitani
AR-NW12	(In-vacuum Type Tapered Undulator)	
A	Macromolecular crystallography	M. Hikita
AR-NW14	(In-vacuum Undulator)	
A	Time-resolved X-ray diffraction, scattering and absorption	S. Nozawa

♥ User group operated Experimental equipment operated by user groups

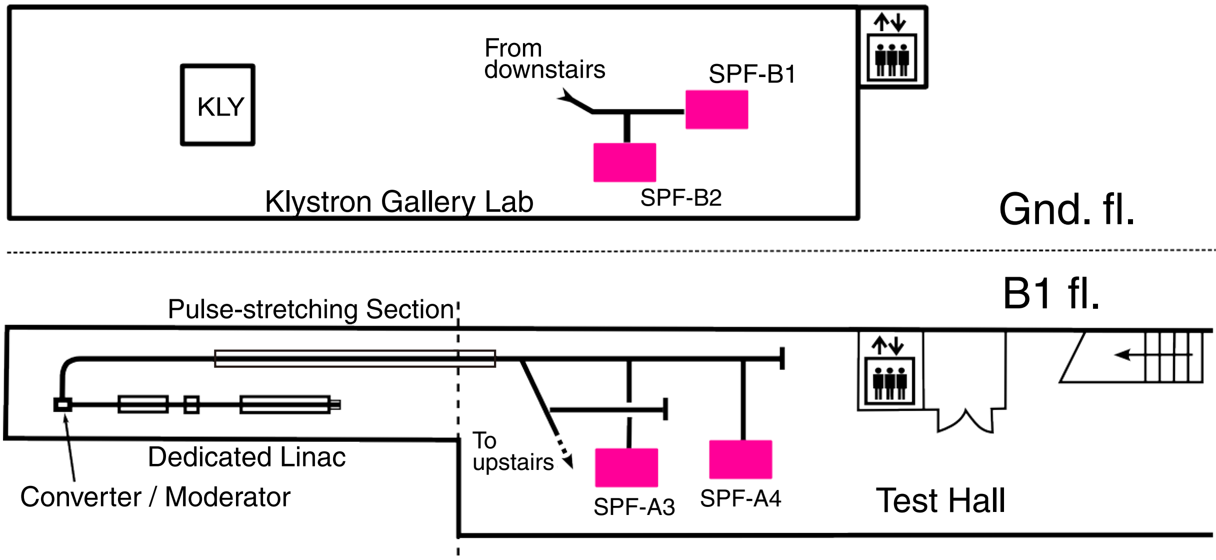

Figure 10: View of the beamlines in the Slow Positron Facility.

Table 9: List of the experimental stations in the Slow Positron Facility.

Experimental Station		Person in Charge
SPF-A3	Total-reflection high-energy positron diffraction	I. Mochizuki
SPF-A4	Low-energy positron diffraction	I. Mochizuki
SPF-B1	General purpose (Positronium laser cooling)	I. Mochizuki
SPF-B2	Positronium time-of-flight	I. Mochizuki

4. Summary of User Proposals

The Photon Factory accepts experimental proposals submitted by researchers mainly at universities and research institutes inside and outside Japan. The PF Program Advisory Committee (PF-PAC) reviews the proposals, and the Advisory Committee for the Institute of Materials Structure Science approves those that are favorably recommended. The number of accepted proposals over the period 2008–2019 is shown in **Table 10**, where S1/S2, U, G, P, and MP denote Special, Urgent, General, Preliminary, and Multi-Probe proposals, respectively. Category T is a proposal for supporting researches by PhD students. Category MP is a proposal in which at least two of the four beams, synchrotron radiation at the PF, slow positron beam at Slow Positron Facility, and neutron and muon beams at the Materials and Life Science Experimental Facility (MLF) in J-PARC, are required to be used, as a multi-probe experiment.

Category C is a proposal for collaboration between KEK and a research institute including a private company. Category I is a non-proprietary proposal for the integrated promotion of social system reform and research and development, supported by the Ministry of Education, Culture, Sports, Science and Technology (from 2009 to 2015).

Category V is a non-proprietary grant-aided proposal that has already been reviewed and approved for a research grant; beam time for proposals in this category is allocated with high priority, and applicants are required to pay the stipulated fees for the beam time. Category Y is a proprietary proposal; applicants are required to pay the stipulated fees for the beam time.

The number of current G-type proposals each year has exceeded 700 for the past few years. In addition to these proposals, 53 projects in the BINDS program (Basis for Supporting Innovative Drug Discovery and Life Science Research) were performed at the PF in FY2019. A full list of the proposals effective in FY2019 and their scientific output can be found in the Photon Factory Activity Report (https://www2.kek.jp/ imss/pf/science/publ/acrpubl.html).

Table 10: Number of proposals accepted for the period 2008–2019.

category	FY-2008	2009	2010	2011	2012	2013	2014	2015	2016	2017	2018	2019
S1	0	0	0	0	0	0	0	0	0	0	1	0
S2	4	6	3	2	4	5	4	7	6	1	6	3
U	3	2	2	0	4	1	0	1	0	0	0	0
G	402	397	407	415	454	447	407	361	372	392	321	350
P	14	14	16	11	18	18	5	16	10	16	16	18
T							6	4	3	3	2	3
MP								3	0	0	1	-
C	18	12	15	19	20	20	25	24	19	21	21	22
I		9	17	13	17	13	16	11	-	-	-	-
V					1	2	2	2	4	4	10	7
Y	22	29	31	30	30	41	22	33	39	30	39	37

S-type proposals consist of two categories, S1 and S2. S1 proposals are self-contained projects of excellent scientific quality, and include projects such as the construction and improvement of beamlines and experimental stations which will be available for general users after the completion of the project. S2 proposals are superior-grade projects that require the full use of synchrotron radiation or long-term beam time. Proposals are categorized into five scientific disciplines, and reviewed by the five subcommittees of PF-PAC: 1) electronic structure, 2) structural science, 3) chemistry and materials, 4) life science I (protein crystallography), and 5) life science II (including soft matter science). **Figure 11** shows the distribution by research field of the proposals accepted by the subcommittees in FY2019.

The number of users for all types of proposals is about 3,000. About 20% of the proposals are conducted by new spokespersons, indicating that the Photon Factory is open to public academic users. **Figure 12** shows the distribution of users by institution and their positions. Over three-quarters of the users belong to universities. About two-thirds of the university users are graduate and undergraduate students, clearly showing the important role that the Photon Factory plays in both research and education. The geographical distribution of the Photon Factory users is shown in **Figs. 13** and **14**, which also indicates the immense contribution of the Photon Factory to research and education throughout Japan. The registered number of papers published in 2019 based on experiments at the PF was 606 at the time of writing (July 1, 2020). In addition, 59 doctoral and 232 master theses have been presented.

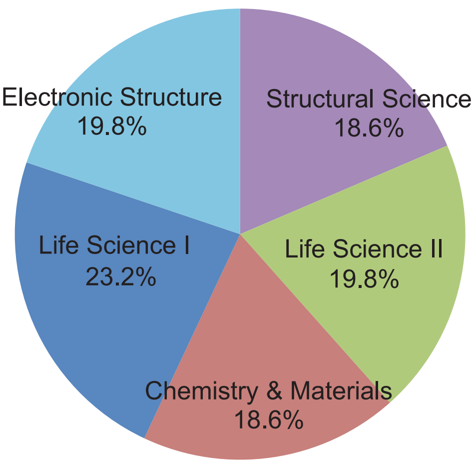

Figure 11: Distribution by scientific field of experimental proposals accepted in FY2019.

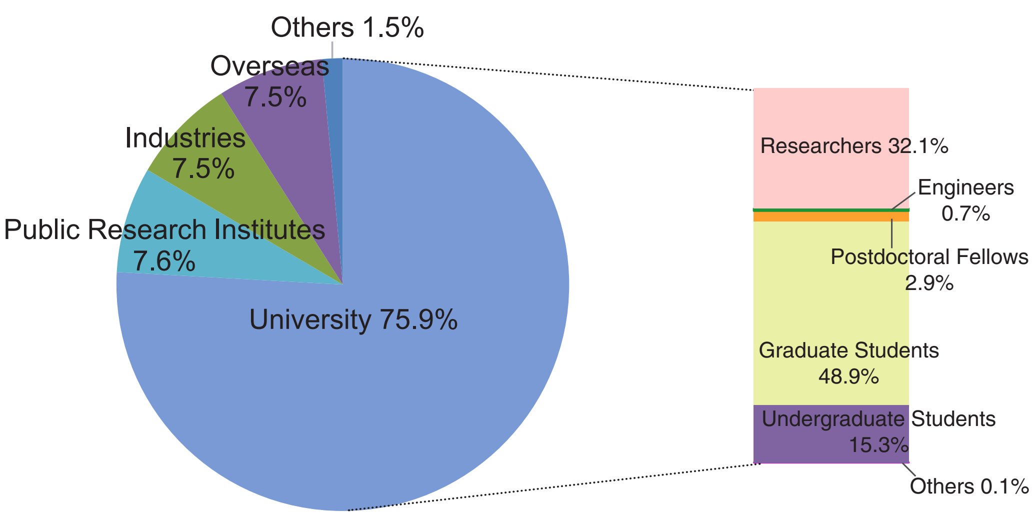

Figure 12: Distribution of users by institution and position.

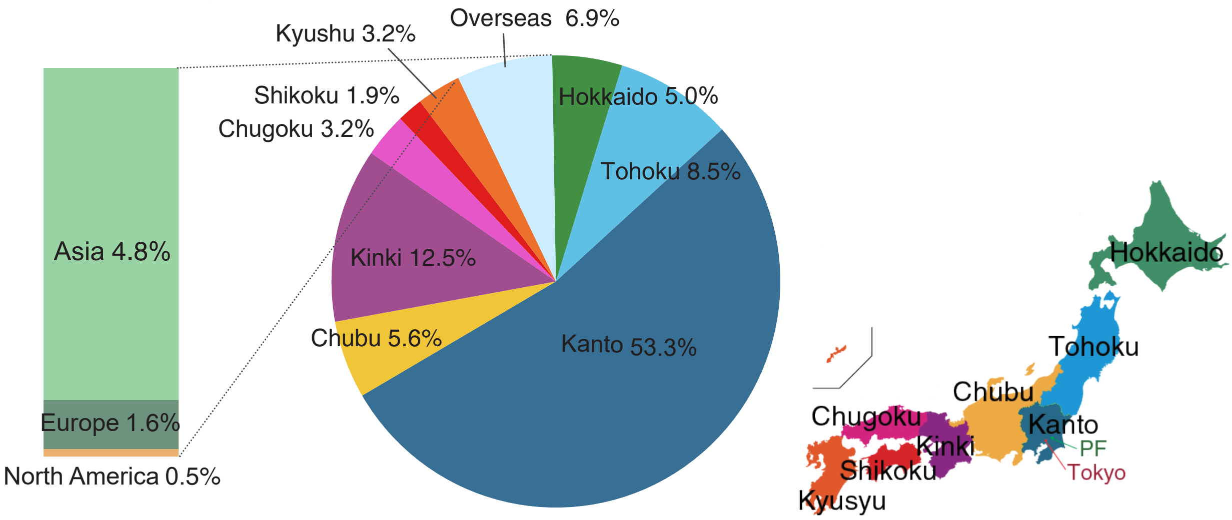

Figure 13: Regional distribution of spokespersons of proposals accepted in FY2019.

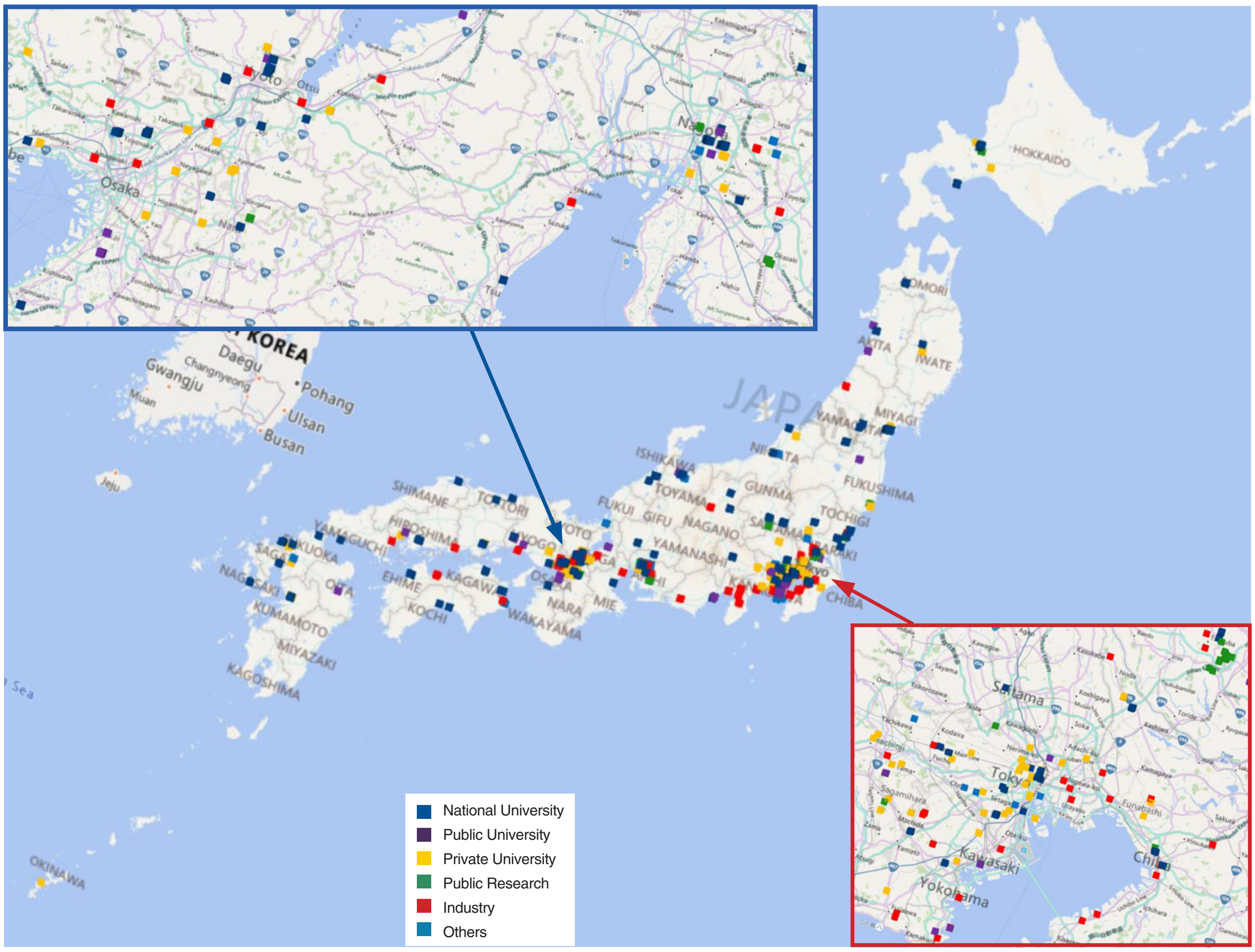

Figure 14: Geographical distribution of Photon Factory users in FY2019 (domestic users only).